RESEARCH REPORTS
Biomaterials & Bioengineering

M. Baldassarri[1,2], H.C. Margolis[1,2], and E. Beniash[1,2*¶]

[1]Department of Biomineralization, The Forsyth Institute, Boston, MA, USA; and [2]Department of Developmental Biology, Harvard School of Dental Medicine, Boston, MA, USA; ¶current address, Oral Biology, University of Pittsburgh School of Dental Medicine, 589 Salk Hall, 3501 Terrace Street, Pittsburgh, PA 15261, USA; *corresponding author, ebeniash@pitt.edu

J Dent Res 87(7):645-649, 2008

Compositional Determinants of Mechanical Properties of Enamel

APPENDICES

APPENDIX 1

To determine whether there is a significant difference between fresh wet and rehydrated freeze-dried enamel, we performed an experiment on human incisor enamel. Human enamel was chosen for technical reasons. Due to the small size of rat incisors, it is impossible to polish them without mounting them in a resin, which would require dehydration. In contrast, it is possible to cut slices of fresh human teeth and polish them as they are, with no need to dry the specimens.

Wet human incisors were sectioned and polished in the same way as described for rat incisors. The hardness of fresh polished samples was tested by means of the microindenter at 0.98 N. Other specimens were freeze-dried in liquid N_2 and lyophilized for 24 hrs. They were then rehydrated in the same way as the rat samples (in a humidity chamber at 37°C and 100% relative humidity for 72 hrs), and their hardness was tested by means of the microindenter at 0.98 N. The hardness values of the fresh wet and freeze-dried rehydrated samples are presented in the Table below. They were compared by a *t* test ($\alpha = 0.05$), and no significant difference was found ($p = 0.69$).

	Hardness Values ($HV_{0.98}$)	
Test Number	Fresh Wet Sample	Rehydrated Freeze-dried Sample
1	397	394
2	364	401
3	345	334
4	397	360
5	383	340
6	383	401
7	360	387
8	408	412
9	370	383
10	416	394
11	416	394
12	408	401
Average	387.3	383.4
Standard deviation	23.6	25.2

APPENDIX 2

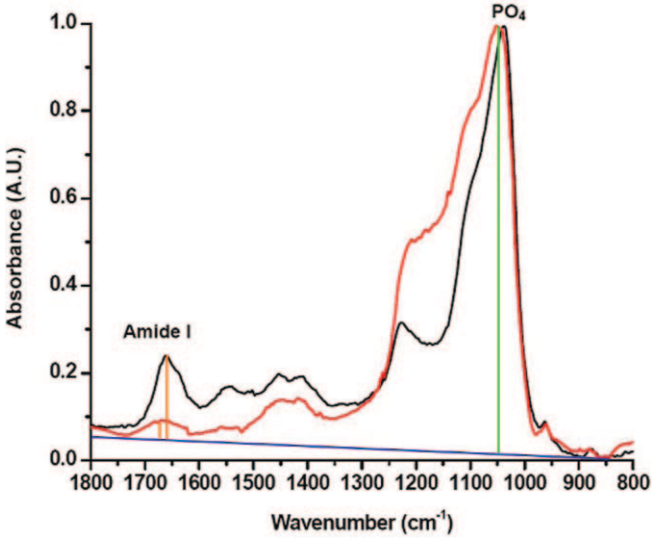

Appendix Figure 1. Reflectance FTIR spectra of murine molar dentin, before (black line) and after (red line) 4 hrs of cold plasma-ashing. After being ashed, the samples were cut transversely and polished to expose deep areas of dentin. The spectra were taken by means of a Multiscope FTIR microscope attached to a Spectrum One FTIR spectrometer (Perkin-Elmer, Shelton, CT, USA) from 50 x 50-μm areas of dentin at least 100 μm from the surface of the sample exposed to the plasma. Spectra were processed according to the Kramers-Kronig transform, designed to convert reflectance data into absorbance-like spectra. The differences in the ratios of peak intensities of amide I (major protein absorbance band) and ν_3 PO_4 were used to monitor organic matrix removal. The amide I absorbance at 1600-1700 cm^{-1} was significantly reduced in the ashed sample, due to protein removal.

APPENDIX 3

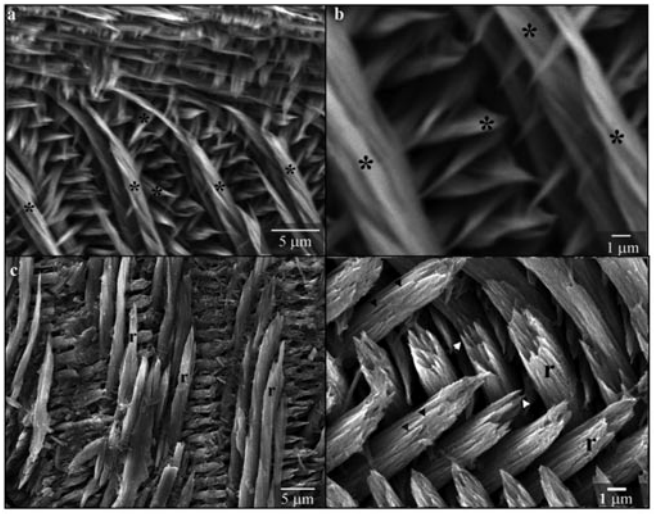

Appendix Figure 2. SEM micrographs of untreated **(a,b)** and plasma-treated **(c,d)** samples. The plasma-treated samples were cut transversely and polished to expose deep regions of enamel. Both plasma-treated and untreated samples were incubated for 30 min in an aqueous solution containing 1% EDTA and 2% glutaraldehyde, with pH adjusted to 6.7. The samples were briefly rinsed in distilled water, air-dried, and sputter-coated with the use of a Pt/Au electrode. The samples were studied in a JEOL 6400 scanning electron microscope (SEM; JEOL, Tokyo, Japan) in a secondary electron mode at 15 kV and working distance of 8 mm. SEM micrographs of untreated enamel (a,b) show the demineralized enamel surface with a thin sheath of organic matrix (asterisks) organized into a typical *quasi*-orthogonal pattern. (c,d) SEM micrographs of plasma-treated enamel taken from the area that was at least 50 µm beneath the surface exposed to the plasma during the treatment. The micrographs show the demineralizing surface of enamel. The individual crystals comprising the enamel rods (r) are indicated by arrowheads.

APPENDIX 4

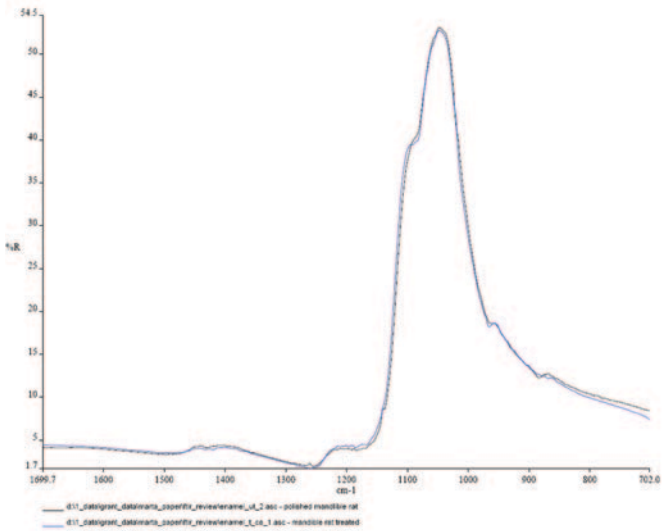

Appendix Figure 3. Reflectance FTIR spectra of murine incisor enamel, before (black line) and after (blue line) 4 hrs of cold plasma treatment. The spectra were taken by means of a Multiscope FTIR microscope attached to a Spectrum One FTIR spectrometer (Perkin-Elmer, Shelton, CT, USA). The major mineral vibration bands, ν_3/ν_1 of PO_4^3 at 1100-900 cm^{-1}, are almost identical in both spectra, suggesting that enamel mineral was not changed by the treatment.

APPENDIX 5

Equations Used to Obtain Hardness and Fracture Toughness Values

For each indentation, hardness and fracture toughness values were computed according to the methods below.

Hardness Computation

For each indentation, the hardness value was determined according to the following formula (ASTM, 1991):

$$HV = 2 * P * \frac{\left(\sin\left(\frac{\theta}{2}\right)\right)}{D^2} = \frac{1.854*P}{D^2}$$

where:
HV = Vickers hardness;
P = applied load = 0.98 N;
θ = angle between opposite faces of diamond = 136°; and
D = indentation diagonal (µm).

Fracture Toughness Computation

The fracture toughness was determined according to a previously described method (Anstis *et al.*, 1981). This equation has been widely used in the literature, primarily due to its simplicity of use and reliability. A recent comparative study of calculations of enamel fracture toughness involving a large number of different equations (Sakar-Deliormanli and Guden, 2006) clearly demonstrated that the equation by Anstis *et al.* is a preferable technique for calculating enamel fracture toughness from microindentation data.

The length of cracks was measured from optical images taken within 5 sec after the mechanical test. For each indentation, a circle enclosing all associated cracks (both edge and side cracks) was drawn, and its radius, developed from the center of the indentation, was taken as the crack length value (c) of that specific indentation (Appendix Fig. 4).

The fracture toughness was computed by means of the

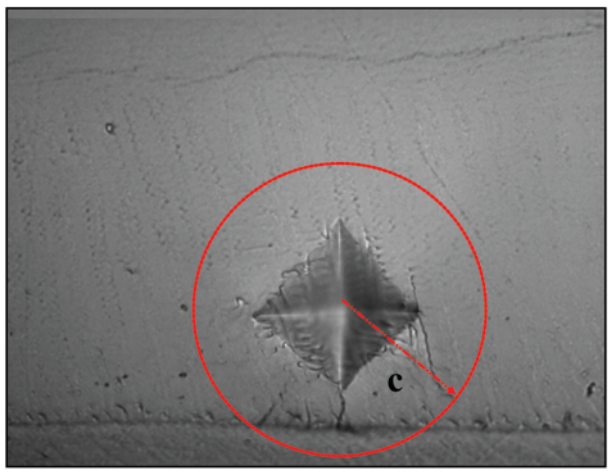

Appendix Figure 4. Light micrograph of a polished murine incisor with the indentation. The red circle encloses all the cracks generated during the indentation. The radius of this circle is used as a crack length measure C.

following equation (Anstis *et al.*, 1981):

$$K_c = 0.0154 * \left(\frac{E}{H}\right)^{1/2} * \left(\frac{P}{c^{1.5}}\right)$$

where:
K_c = fracture toughness ($MPa*m^{1/2}$);
0.0154 = calibration constant (Anstis *et al.*, 1981);
E = elastic modulus (GPa) (84.1) (Craig *et al.*, 1961);
H = hardness (GPa) = measured hardness value from each indentation was converted from HV to GPa and included in the K_c formula;
P = applied load = 0.98 N; and
c = crack length (μm) from the center of the indentation impression (Anstis *et al.*, 1981).

APPENDIX REFERENCES

Anstis GR, Chantikul P, Lawn BR, Marshall DB (1981). A critical evaluation of indentation techniques for measuring fracture toughness: I. Direct crack measurements. *J Am Ceram Soc* 64:533-538.

ASTM (1991). ASTM designation E 384. In: Standard test method for microhardness of materials. Philadelphia: American Society for Testing and Materials.

Craig RG, Peyton FA, Johnson DW (1961). Compressive properties of enamel, dental cements, and gold. *J Dent Res* 40:936-945.

Sakar-Deliormanli A, Guden M (2006). Microhardness and fracture toughness of dental materials by the indentation method. *J Biomed Mater Res B Appl Biomater* 76:257-264.